Vortex fractionalization in a Josephson ladder

I. Tornes* and D. Stroud†
Department of Physics, The Ohio State University, Columbus, Ohio 43210, USA
(Received 17 August 2005; revised manuscript received 7 November 2005; published 30 December 2005)

We show numerically that, in a Josephson ladder with periodic boundary conditions and subject to a suitable transverse magnetic field, a vortex excitation can spontaneously breakup into two or more fractional excitations. If the ladder has N plaquettes, and N is divisible by an integer q, then in an applied transverse field of $1/q$ flux quanta per plaquette the ground state is a regular pattern of one fluxon every q plaquettes. When one additional fluxon is added to the ladder, it breaks up into q fractional fluxons, each carrying $1/q$ units of vorticity. The fractional fluxons are basically walls between different domains of the ground state of the underlying $1/q$ lattice. The fractional fluxons are all depinned at the same applied current and move as a unit. For certain applied fields and ladder lengths, we show that there are isolated fractional fluxons. It is shown that the fractional fluxons would produce a time-averaged voltage related in a characteristic way to the ac voltage frequency.

DOI: 10.1103/PhysRevB.72.224519 PACS number(s): 74.81.Fa, 74.50.+r, 74.25.Qt

I. INTRODUCTION

Ladder arrays of Josephson junctions have been extensively studied both theoretically and experimentally (see, for example, Refs. 1–15). They are of interest, in part, because they show a rich variety of equilibrium and dynamical behavior. In addition, they are an important testing ground for concepts of phase transitions and quantum behavior in lower dimensionality. The interest in such materials is even greater now, because advances in microfabrication allow such ladders to be made almost to specifications, in order to test theoretical predictions or possibly to make types of Josephson devices.

Recently Chandran and Kulkarni[16] considered the behavior of a hypothetical Josephson ladder array with alternating π and 0 junctions. A π junction is one in which the Josephson supercurrent $I=I_c \sin(\Delta\phi+\pi)$, where $\Delta\phi$ is the phase difference across the junction and $I_c>0$. Such junctions can be formed in a variety of ways, e.g., by controlling the energy distribution of the current-carrying states in the normal metal within the junction,[17] by preparing a junction between two cuprate superconductors in the presence of bound states in the interface material,[18] or by connecting two superconductors across a ferromagnetic layer.[19] Thus, an array of alternating 0 and π junctions could, in principle, be made in the laboratory. In Ref. 16, it was shown that when a 2π fluxon is introduced into such a $0-\pi$ ladder, it will break up into two separate π fluxons, each of magnitude $\Phi_0/2$. This fractionalized vortex was predicted to have unusual current-voltage characteristics which could readily be detected experimentally.

In this paper, we show that similar fractionalized vortices are produced in *conventional* ladder Josephson arrays made of 0 junctions, in a transverse magnetic field. Specifically, we consider a ladder having N square plaquettes, where N is divisible by an integer q, in a transverse magnetic field. If that field is of magnitude equal to one flux quantum per q plaquettes, the ground state of the ladder is a periodic array of N/q equally spaced fluxons. If now one fluxon is added to that ladder, we find that the added fluxon breaks up into q fractional fluxons, each of magnitude Φ_0/q. If $q=2$, the fluxon pattern is similar to that found in Ref. 16, but we find analogous patterns for all other values of q which we have tested. These extra fluxons have I-V characteristics and vorticity patterns which should be readily detectable experimentally. Furthermore, the fractionalized fluxons are typically "confined" that is, they are typically depinned at the same current and move at the same velocity. For an array in which N is not divisible by an integer q, we show numerically that it is possible to produce *isolated* fractional fluxons, by applying a transverse magnetic field of suitable magnitude.

The remainder of this paper is arranged as follows. In Sec. II, we develop the equations of motion from a standard Lagrangian for the Josephson ladder. In Sec. III, we give our numerical results, which show that fractional vortices are generated in the ladder at suitable applied transverse fields. Finally, in Sec. IV, we briefly compare our results to other models which give rise to fractional excitations, and give a concluding discussion.

II. FORMALISM

We consider a Josephson ladder with periodic boundary conditions, as shown schematically in Fig. 1. The ladder is assumed to consist of a collection of small junctions, each of critical current I_c, which are inductively coupled together. The edges of the ladder are parallel to the x axis, while the rungs are in the y direction. A dc current I is injected into each junction on one edge of the ladder and extracted from each junction on the other edge. A magnetic field $\mathbf{B}=B\hat{\mathbf{z}}$ is applied perpendicular to the ladder. The geometry is readily achievable experimentally, in the form of a coplanar ring perpendicular to $\mathbf{B}$.

In the absence of dissipation, it is convenient to describe the ladder by the following Lagrangian

$$\mathcal{L}=K-V, \tag{1}$$

where

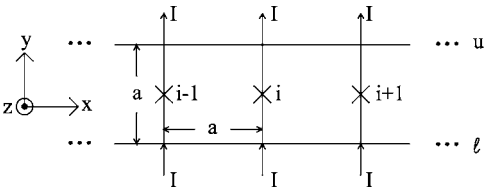

FIG. 1. Schematic of the ladder modeled in this paper. We show the $i-1$, i, and $i+1$ rungs. u and ℓ denote the upper and lower edges of the ladder. An external magnetic field is applied in the $\hat{\mathbf{z}}$ direction; a dc driving current I is applied to the lower end of each rung in the $\hat{y}$ direction and extracted from the upper end. The ladder is assumed to have the topology of a ring (periodic boundary conditions). The full lines along the upper and lower edges of the ladder (parallel to x) are treated simply as inductors in our model.

$$K = \sum_{i=1}^{N} \frac{\hbar^2}{2U}(\dot{\theta}_{i,u} - \dot{\theta}_{i,\ell})^2 \tag{2}$$

and

$$V = \sum_{i=1}^{N} [-J_1 \cos(\theta_{i,\ell} - \theta_{i,u} - A_i) + J_2(\theta_{i,\ell} - \theta_{i+1,\ell})^2 + J_2(\theta_{i,u} - \theta_{i+1,u})^2 - J_3(\theta_{i,u} - \theta_{i,\ell} - A_i)]. \tag{3}$$

Here K represents the charging energy of the small junctions, $U=4e^2/C$, and C is the capacitance of the small junction. $J_1=\hbar I_c/2e$ is the Josephson coupling energy of the small junction, $J_3=\hbar I/(2e)$, and $J_2=\hbar^2/(8e^2L)$, where L is the inductance of the wire segments coupling points (i,ℓ) to $(i+1,\ell)$ and (i,u) to $(i+1,u)$. Finally, if we use the gauge $\mathbf{A}=Bx\hat{\mathbf{y}}$, where $\mathbf{A}$ is the vector potential, then $A_i=(2\pi/\Phi_0)\int_{i,\ell}^{i,u}\mathbf{A}\cdot\mathbf{dl}=(2\pi/\Phi_0)a^2iB$, where $\Phi_0=hc/(2e)$ is the flux quantum, a is the lattice constant (see Fig. 1), and the subscripts ℓ and u indicate the lower and upper ends of the junction, as shown in the figure. The dots indicate time derivatives. Note that we neglect the self-induced magnetic field, by taking B equal to the externally applied field.

If we now make the substitutions $\phi_i=\theta_{i,u}-\theta_{i,\ell}$, $\chi_i=(\theta_{i,\ell}+\theta_{i,u})$,[3,12] we may reexpress the Lagrangian as

$$\mathcal{L} = \sum_{i=1}^{N} \left\{ \frac{E_C}{2}\dot{\phi}_i^2 + J_1\cos(\phi_i - A_i) + J_3\phi_i + -\frac{J_2}{2}[(\chi_i - \chi_{i+1})^2 + (\phi_i - \phi_{i+1})^2] \right\}. \tag{4}$$

The Lagrange equations of motion are then $[d/dt(\partial\mathcal{L}/\partial\dot{\phi}_i)] = \partial\mathcal{L}/\partial\phi$, with an analogous equation for the variables χ_i. Since $\mathcal{L}$ is independent of $\dot{\chi}_i$, the equation of motion for χ_i leads to the condition that $\chi_i-\chi_{i+1}$ is independent of i. After some algebra, it is readily shown that the equation of motion for ϕ_i is

$$\ddot{\phi}_i = -\sin(\phi_i + 2\pi i f) + \lambda_J^2(\phi_{i-1} - 2\phi_i + \phi_{i+1}) + (I/I_c) - \dot{\phi}_i/Q_J. \tag{5}$$

Here, we have introduced the frustration $f=Ba^2/\Phi_0$, and a dimensionless time $\tau=\omega_p t$, where $\omega_p=[2eI_c/(\hbar C)]^{1/2}$ is the junction plasma frequency, and $\lambda_J=(J_2/J_1)^{1/2}$ is a dimensionless Josephson penetration depth. The dot now represents a derivative with respect to τ. Finally, we have added an additional dissipative term $-\dot{\phi}_i/Q_J$ by hand to the equation of motion, where Q_J is a dimensionless junction quality factor, assumed to be the same for all junctions. In the resistively and capacitively shunted junction model (RCSJ),[20] $Q_J=(2eR^2I_cC/\hbar)^{1/2}$, where R is the junction shunt resistance.

III. NUMERICAL RESULTS

A. Numerical method

In most of our calculations, we have studied a ladder with $N=120$ rungs and periodic boundary conditions. This number of rungs was chosen because it is the smallest integer divisible by 2, 3, 4, 5, and 6, and is sufficiently large to allow the fractionalization to be apparent in the simulations. We solved our set of 240 first order, nonlinear, differential equations using a constant-time-step, fourth-order Runge-Kutta method.[21] We have generally considered underdamped junctions, with $Q_J=10$, and values of λ_J^2 between 0.01 and 10. We initialized the system in a random phase configuration at $\tau=0$ and $I/I_c=0$. The equations are integrated forward in time up to $\tau_{eq}=3000$, by which time we assume the system has reached a steady state. We then calculate the time-averaged voltage drop across a rung of the ladder (also averaged over the rungs) by averaging over an additional $\tau_{max}-\tau_{eq}$ dimensionless time units, i.e.,

$$\frac{\langle V\rangle}{RI_c} = \frac{1}{NQ_J(\tau_{max}-\tau_{eq})}\sum_{i=1}^{N}\int_{\tau_{eq}}^{\tau_{max}}\frac{d\phi_i}{d\tau}d\tau, \tag{6}$$

where $\tau_{max}=5000$. The dc driving current is then increased by $0.01I_c$ and the calculation is repeated. We continue ramping up the current by steps of 0.01 until $I/I_c=1.2$, then decrease I/I_c in steps of 0.01 back to zero. These calculations give the I-V curves shown below in Figs. 2(a), 5, 7, and 9.

B. $f=1/2$

In Fig. 2(a), we show the full I-V curve for $f=1/2$, $Q_J=10$, and $\lambda_J^2=1$. The directions of the arrows indicate whether the current is increasing or decreasing. The I-V curve is clearly hysteretic for this value of Q_J, and has two discontinuous jumps on the increasing current branch. At the lower jump, near $I/I_c=0.13$, the system jumps into a state where the fluxon lattice is depinned and starts to move through the ladder as a unit, giving rise to a finite voltage across the ladder. At the upper jump, near $I/I_c=0.5$, all the junctions switch to a finite voltage state and the fluxon excitations are expelled from the ladder.

To represent the fluxon lattice pictorially, we use the concept of a *vortex number*.[22] The vortex number of the αth plaquette is defined as

$$n_\alpha = f + \frac{1}{2\pi}\sum_{\text{plaquette}}(\theta_i - \theta_j - A_{ij}). \tag{7}$$

Here the gauge-invariant phase difference for each leg of the plaquette is written $(\theta_i-\theta_j-A_{ij})$ and is defined to lie in the

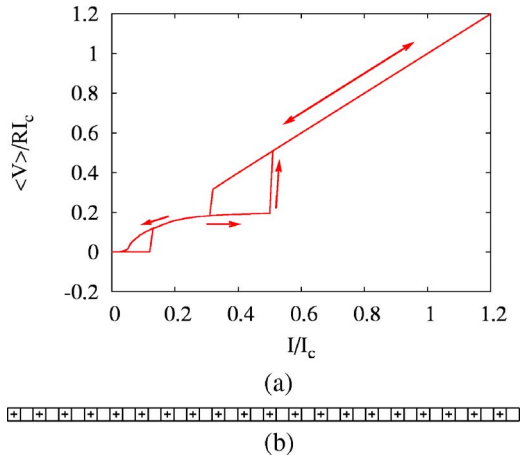

FIG. 2. (Color online) (a) I-V curves for $f=1/2$, $Q_J=10.0$, and $\lambda_J^2=1.0$ for increasing and decreasing current (the directions are indicated by arrows). There are two voltage jumps in the I-V curve on the increasing branch: at the first, the fluxon lattice is depinned; at the second, the junctions switch to the voltage state. (b) Schematic of ground state vortex number configuration for the $f=1/2$ ladder at $I/I_c=0$; the +'s and blank squares represent vortex numbers $n=1$ and $n=0$. Only 40 plaquettes are shown.

range $[-\pi,\pi]$; the summation is taken around the plaquette in the counterclockwise direction (viewed from the positive z axis). Thus n_α is 0 or a positive or negative integer for each plaquette. In the lowest energy state, we expect that $\Sigma_\alpha n_\alpha = Nf$, where N is the number of plaquettes, and also that all the individual $n_\alpha=0$ or 1.

The two values of n_α can generally be distinguished by the current pattern around the plaquette: $n_\alpha=1$ and 0 correspond to a clockwise and counterclockwise current flow, respectively. The expected ground state for $f=1/2$ at $I/I_c=0$ is shown pictorially in Fig. 2(b). The +'s and empty squares represent plaquettes of $n_\alpha=1$ and 0, respectively.

In practice, we have not found a way to calculate n_α directly, because we do not compute the variables χ_i mentioned above. Therefore, in order to confirm the vortex pattern at various fields and currents, we calculate the "normalized flux," defined by the relation $2\pi\Phi_i/\Phi_0=\phi_i-\phi_{i+1}+2\pi f$, in each plaquette. We show a number of examples of this normalized flux below.

When the vortex lattice is depinned near $I/I_c=0.13$, the entire lattice of +'s moves as a unit through the ladder, generating a voltage. In Fig. 3, we show the space-averaged voltage

$$\frac{V(\tau)}{RI_c}=\frac{1}{NQ_J}\sum_i^N \dot{\phi}_i(\tau) \tag{8}$$

across the ladder for $4500<\tau<4520$, for the parameters of Fig. 2(a) at $I/I_c=0.13$, just above the lower jump in the I-V characteristics. We interpret the periodic voltage oscillations as arising from the motion of the fluxon lattice through the bumpy "egg-carton" potential provided by the plaquettes of the Josephson ladder: the velocity of the fluxon lattice varies periodically in time because the fluxon lattice moves alternately faster and slower as it moves through the steeper and less steep part of the egg carton.[23]

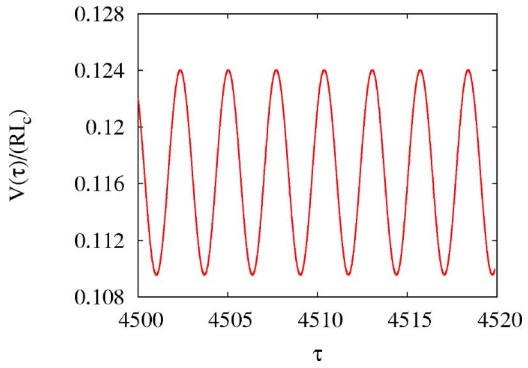

FIG. 3. (Color online) Time-dependent voltage $V(\tau)/(RI_c)$ across one rung of the ladder, averaged over the rungs, and plotted for dimensionless time τ between 4500 and 4520, for $f=1/2$ and the parameters of Fig. 2(a). The dimensionless period of voltage oscillation is ~ 2.7 at $I/I_c=0.13$.

To confirm this picture, we note from Fig. 3 that the dimensionless period of the voltage oscillation, which we denote $\Delta\tau$, is ~ 2.7. We expect that this should be the dimensionless time required for the fluxon lattice to advance one lattice constant a. Now if the fluxon lattice moves a distance a during this period, then the average speed of the fluxon lattice is $v=(Na)/T$, where T is the time required for the lattice to complete one circuit around the ladder. During this time, each junction should experience a phase change of $2\pi Nf$, since Nf fluxons cross each junction during one circuit. Thus, the time-averaged voltage $\langle V\rangle$ across each junction should be $[\hbar/(2e)]2\pi Nf/T$. Introducing a dimensionless voltage $\langle V\rangle/(RI_c)$, and noting that the time required to move one lattice constant a is $\omega_p T/N=\Delta\tau$, we obtain

$$\frac{\langle V\rangle}{RI_c}=\frac{2\pi f}{Q_J\Delta\tau}. \tag{9}$$

Using the parameters of Fig. 2(a), together with $I/I_c=0.13$ and $\Delta\tau=2.7$, Eq. (9) gives $\langle V\rangle/(RI_c)=2\pi(1/2)/(10\times 2.7)=0.116$. The actual time-averaged voltage read off from Fig. 2(a) at $I/I_c=0.13$ is 0.117, in excellent agreement with this calculated value. Thus, the time-dependent voltage shown in Fig. 3 is consistent with the picture of a fluxon lattice moving as a unit through the washboard potential provided by the ladder. For currents slightly higher than $I/I_c=0.13$, this picture of a moving vortex lattice continues to hold. As the current is increased still further, for $Q_J=10$, the voltage is no longer perfectly periodic in time (not shown in the figure). For I/I_c greater than about 0.51, the individual junctions switch to a voltage state and the moving fluxon lattice disappears.

In Fig. 4, we plot the calculated normalized flux Φ_i/Φ_0 for $f=1/2$ and $I/I_c=0$. Clearly, Φ_i/Φ_0 alternates between two values, indicating that the flux lattice is periodic with a period of two unit cells, as suggested by Fig. 2(b). The two ground state fluxes are approximately $2\pi f\pm f$ with $f=1/2$. A similar pattern has been seen previously in Ref. 16 for a

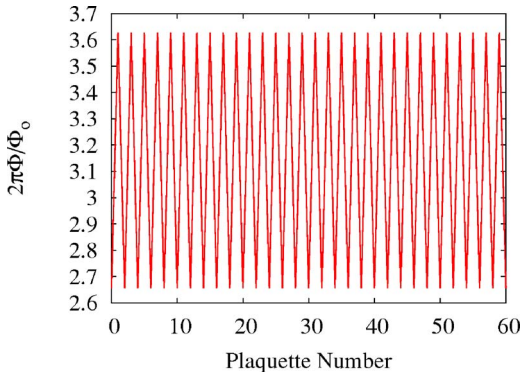

FIG. 4. (Color online) Normalized "flux" $2\pi\Phi_i/\Phi_0$ (as defined in the text) vs plaquette number i, for the parameters of Fig. 2(a) and $I/I_c=0$. For clarity, only 60 of the 120 plaquettes are shown.

ladder with alternating 0 and π junctions, and zero applied magnetic field.

C. $f=1/2+1/N$

Next, we consider the case $f=1/2+1/120$, equivalent to adding one fluxon to the $f=1/2$ ladder. The calculated results are shown in Figs. 5 and 6. Figure 5 shows the I-V characteristic as computed on increasing and decreasing the current in steps of $0.01I_c$. On the increasing branch, there are now three steps in the I-V curve. Two of the steps are easily seen from the figure, but the lowest jump, which occurs near $I/I_c=0.01$, is less visible and shown in the inset for $0<I/I_c<0.15$. The I-V curve is hysteretic in two regions of current, but non-hysteretic at the lowest nonzero voltages. On the decreasing branch there are still three distinct regimes of nonzero voltage. We interpret these as follows: (i) at the lowest currents, a single fluxon is depinned and moves through the fluxon lattice formed by the remaining 60 fluxons; (ii) at higher currents, the fluxon lattice is depinned, as at $f=1/2$, generating a larger voltage; and finally (iii) at still higher voltage, all the junctions switch to a voltage state and the ladder jumps up to the resistive branch.

Figure 6(a) shows the flux pattern $2\pi\Phi_i/\Phi_0$ for $f=61/120$ and $I/I_c=0$, keeping the rest of the parameters the same as in Fig. 2(a). The $f=1/2$ pattern is now distorted in *two* regimes, near $i=50$ and $i=110$, while in the rest of the ladder the pattern is similar to that of $f=1/2$. To compare the two patterns more quantitatively, we note that the sums $\Sigma_i\Phi_i/\Phi_0$ for Figs. 4 and 6(a) are $60(2\pi)$ and $61(2\pi)$, respectively. This result shows that the effect of the additional magnetic field is to add one additional fluxon to the ladder. However, this fluxon does not enter the ladder *as a unit*. Instead, it is fractionalized into *two* 1/2 fluxons, each of which carries 1/2 a unit of flux. These two 1/2 fluxons obviously repel one another, since they prefer to be situated as far away from one another as possible, i.e., about 60 plaquettes apart in the 120-plaquette ladder.

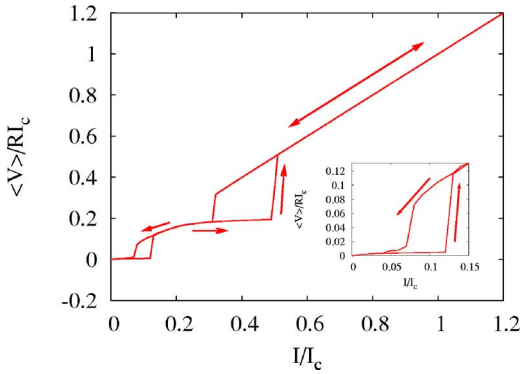

FIG. 5. (Color online) I-V curve for $f=61/120$, $Q_J=10$, and $\lambda_J^2=1$ for increasing and decreasing current (as indicated by arrows). The inset shows the I-V curve for $0<I/I_c<0.15$. A finite voltage in this regime is produced by the two moving 1/2 fluxons.

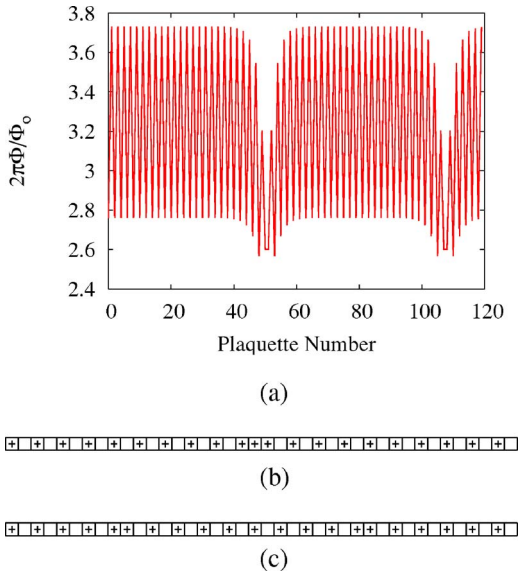

FIG. 6. (Color online) (a) Normalized flux vs plaquette number for the parameters of Fig. 2, except that $f=61/120$. (b) Schematic of an unfractionalized, high-energy vortex charge configuration for $f=61/120$. (c) Schematic of the actual ground state vortex charge configuration at $f=61/120$ and $I/I_c=0$. In both (b) and (c), we show only 40 of the 120 plaquettes. (In the actual ladder, the two fractional vortices are separated by 60 plaquettes.)

To suggest intuitively why the extra fluxon fractionalizes in the ladder, we show in Figs. 6(b) and 6(c) two possible scenarios for how the extra fluxon enters the ladder. In Fig. 6(b), the fluxon enters as a unit, without distorting the underlying $f=1/2$ fluxon lattice. But this scenario leads to $n=1$ vortices in three consecutive plaquettes, as indicated by the three adjacent plus signs. This is obviously a high energy state, since vortices of like signs repel one another. A more plausible state is shown in Fig. 6(c), where the extra fluxon has fractionalized into two 1/2 fluxons. In this case, there are only two points in the ladder where there are two adjacent + signs, and none with three. Our numerical simulations indicate that this is indeed a lower energy state than the unfractionalized fluxon shown in Fig. 6(b). We have also found that both halves of the fractionalized fluxon are depinned at the same I/I_c, and move together.

Finally, we consider the expected time-dependent voltage for the two moving 1/2 fluxons in the 61/120 ladder. As explained above, each 1/2 fluxon is really a kind of domain

wall, consisting of two adjacent + vortex charges. The expected mechanism by which a 1/2 fluxon moves is that one of the two adjacent + charges moves to the nearest empty plaquette. This jump causes the domain wall to move by *two* plaquettes. Thus, if the ladder has length N plaquettes, a 1/2 fluxon will circulate around the ladder *twice* in N moves. This causes a phase slip of 2π, since there is a π phase slip each time the 1/2 fluxon circulates once around the ladder. Thus, if T is the time required for the 1/2 fluxon to circulate once around the ladder, the time-averaged voltage is $\langle V\rangle = (\hbar/2e)\pi/T$. On the other hand, $V(t)$ for a single 1/2 fluxon should have an ac component with a period of $1/\nu = 2T/N$, where ν is the ac frequency, since $2T/N$ is the time required for a 1/2 fluxon to make a single move of two plaquettes.

Combining these two relations, we get $\langle V\rangle = [h/(2eN)]\nu$ for a single 1/2 fluxon. This is precisely the relation between $\langle V\rangle$ and ν which we find for a ladder containing a single 1/2 fluxon, as is discussed later in this paper.

For the present case of a 61/120 ladder, there are, as already mentioned, *two* 1/2 fluxons, as shown in Fig. 6. Thus, at a current I in the regime where the *two* 1/2 fluxons are moving, we expect that $\langle V\rangle$ will equal twice this value, or

$$\langle V\rangle = 2[h/(2eN)]\nu, \tag{10}$$

where ν represents the frequency of the ac voltage generated by a the motion of a single 1/2 fluxon at the same current. We can rewrite this equation in terms of Q_J and $\Delta\tau \equiv \omega_p/\nu$ with the result

$$\frac{\langle V\rangle}{RI_c} = \frac{2(2\pi)}{NQ_J\Delta\tau}. \tag{11}$$

In the present case $N=120$ so the right-hand side equals $2\pi/(60Q_J\Delta\tau)$. The calculated $\langle V\rangle$, in the regime where the two 1/2 fluxons are moving, agrees very well with the prediction of Eq. (11). Thus, the I-V characteristics in this regime are produced by two 1/2 fluxons moving with the same average velocity.

D. $f=1/3$

If an added fluxon fractionalizes when added to a ladder at $f=1/2$, what happens at other values of f? To answer this question, we have carried out similar calculations for 1/3, 1/4, 1/5, and 1/6 in an $N=120$ ladder, as well as for each of these values of f with one fluxon added or subtracted. The calculated I-V characteristics and normalized flux for $f=1/3$ are shown in Figs. 7 and 8(a). The behavior of the I-V curves shown in Fig. 7 is most easily understood on the decreasing current branch. For the highest currents, the junctions are all in the voltage state, and the fluxon lattice has disappeared. At intermediate currents, the $f=1/3$ fluxon lattice is moving through the washboard potential provided by the ladder. At the lowest currents, the fluxon lattice is pinned and the time-averaged voltage vanishes. On the increasing current branch, the fluxon lattice appears to depin in two stages, corresponding to the two voltage jumps visible in Fig. 7.

Figure 8(a) shows the normalized flux Φ_i/Φ_0 versus plaquette number i at $I/I_c=0$ and Fig. 8(b) shows the vortex charge pattern configuration in the equilibrium state. The flux pattern is again periodic, as at $f=1/2$, but now with a period of three plaquettes, with fluxes $2\pi f+f$, $2\pi f+f$, and $2\pi f-2f$.

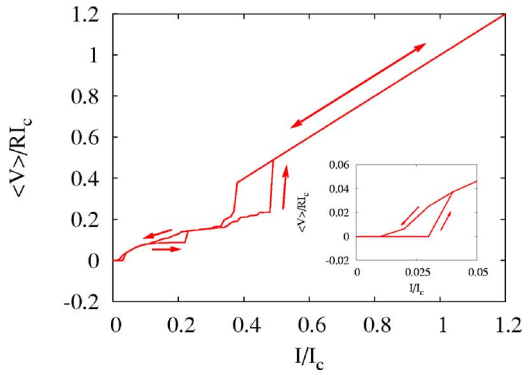

FIG. 7. (Color online) I-V curve for $f=1/3$, $Q_J=10.0$, $\lambda_J^2=1.0$, and $N=120$. The inset shows the I-V curve for $0<I/I_c<0.05$.

As a further check that the fluxon lattice really moves as a unit, we have used Eq. (9) to compare the time-averaged voltage $\langle V\rangle$ at $I/I_c=0.04$, on the upward current sweep just above the first voltage jump, to the dimensionless period $\Delta\tau$ of the ac component. The prediction for $\langle V\rangle/(RI_c)$ from Eq. (9) [namely $\langle V\rangle/(RI_c)=0.0381$] is in excellent agreement with the value calculated by a direct time-average of $\langle V\rangle/(RI_c)$ (0.0372).

E. $f=1/3+1/N$

Next, we consider the behavior of the same system with one additional fluxon. Figure 9 shows the I-V curve, and Fig. 10(a) displays the normalized flux versus the plaquette number at $I/I_c=0$, for $f=1/3+1/120$. In this case, the additional fluxon fractionalizes into *three* excitations. These are visible in Fig. 10(a) as regions which are distorted, in comparison to the flux plot at $f=1/3$. As in Fig. 6(a), these regions show

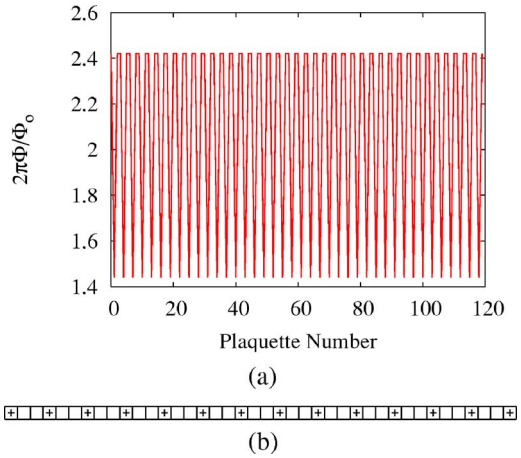

FIG. 8. (Color online) (a) Normalized flux vs plaquette number for the parameters of Fig. 7. (b) Ground state vortex charge configuration for the same parameters as (a), Only 40 of the 120 plaquettes are shown.

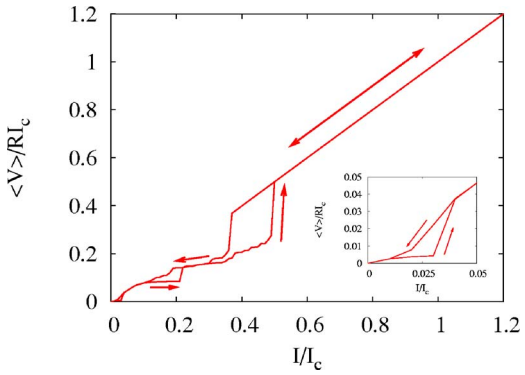

FIG. 9. (Color online) I-V curve for $f=41/120$, $Q_J=10.0$, $\lambda_J^2=1.0$, and $N=120$. There are three jumps on the increasing-current branch of the I-V characteristics; the first occurs near $I/I_c=0.01$, and the others can be easily seen in the figure. The inset shows the I-V curve for $0<I/I_c<0.05$. The interpretation of these regimes is given in the text.

how the $f=1/3$ flux pattern changes to accommodate the additional flux quantum. To understand why this extra fluxon fractionalizes into three parts, we show in Figs. 10(b) and 10(c) two possible patterns of vortex number when the additional fluxon is added. The $f=1/3$ ground state consists of a +1 vortex every three plaquettes. If the additional fluxon is unfractionalized, we expect that it will enter the ladder as in Fig. 10(b). This pattern must have two neighboring plaquettes with a +1 vortex number, and hence, is a relatively high-energy state. It is much more plausible that the lowest-energy pattern would never have +1 vortices in adjacent plaquettes. Such a pattern is shown in Fig. 10(c). The

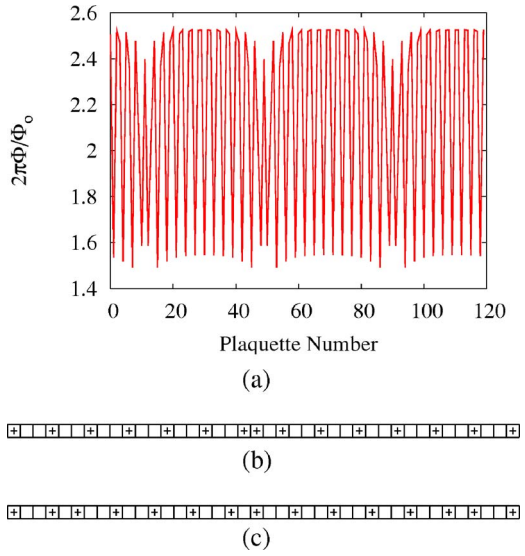

FIG. 10. (Color online) (a) Normalized flux vs plaquette number for the same parameters as in Fig. 7, except that $f=41/120$. (b) A possible high-energy vortex charge configuration for this field. (c) Schematic of the actual ground-state vortex charge configuration, as obtained after iterating the equations of motion up to a time $\tau_{max}=5000$ and $I/I_c=0$. In both (b) and (c), we show only 40 of the 120 plaquettes. In the actual ladder at $f=41/120$, the three 1/3 fluxons are separated by 40 plaquettes, as suggested in Fig. 10(a).

1/3 fluxon shows up as a region where two +1 vortices are separated by only one empty plaquette, rather than two as in the unperturbed $f=1/3$ pattern. To conserve the number of +1 plaquettes, there must be three such regimes; hence, the added fluxon is expected to fractionalize into three 1/3 fluxons, as we find numerically. These 1/3 fluxons are equidistant in order to minimize the repulsive energy between these added excitations.

When the extra fractionalized fluxon moves through the lattice, it generates voltage. Once again, we can use the analog of Eq. (11) to connect the time-averaged voltage to the oscillation period of $V(\tau)$. This analog is

$$\frac{\langle V\rangle}{RI_c}=\frac{3(2\pi)}{NQ_J\Delta\tau}. \tag{12}$$

Here $\Delta\tau$ is now the period of the ac voltage in the regime where three 1/3 fluxons are moving, measured in units of $1/\omega_p$. When we use this relation to calculate $\langle V\rangle$ from our calculated $\Delta\tau$, at $I/I_c=0.02$ (in the regime of three moving 1/3 fluxons), we find that the value of $\langle V\rangle$ obtained from Eq. (12), using the calculated value of $\Delta\tau$ is in excellent agreement with the value of $\langle V\rangle$ calculated directly.

F. $f=1/q$ and $f=1/q+1/N$, with $q>3$

We have also carried out similar calculations for 1/4, 1/5, and 1/6. The ground state (at $I/I_c=0$) consists, as expected, of a periodic array of +1 vortices separated by $q-1$ zero vortices ($q=4$, 5, or 6). When we carry out the corresponding calculations for $f=1/4+1/N$, $f=1/5+1/N$, and $1/6+1/N$, we again find that the added vortex fractionalizes into q equally spaced pieces, as suggested by our results for $q=2,3$.

G. Effects of varying ladder length, inductive coupling, and damping coefficient. Effects of removing one fluxon

We have also studied $f=1/q+1/N$ ($q>1$) for a ladder of double the length, i.e., 240 plaquettes. The flux patterns are very similar to those of the shorter ladders, except that, of course, the fractionalized fluxons are twice as far apart as for $N=120$; the I-V curves are also qualitatively similar.

As another important test case, we have computed both the ground state configurations and I-V characteristics for $f\rightarrow f-1/N$, in order to compare the effects of *removing* rather than adding one fluxon. (We do not display these results graphically.) In general, the results are similar to those found for adding one fluxon. The results for $f=1/2-1/N$ are nearly identical to those for $f=1/2+1/N$: the missing fluxon is fractionalized into two half-fluxons. For $f=1/q-1/N$, with $q>1$ an integer, the I-V and flux characteristics are similar to those for $f=1/q+1/N$; however, the flux curves are not identical, except for $q=2$. It is not surprising that one obtains different results for adding and subtracting a fluxon for $q>2$: only at $q=2$ would one expect, on symmetry grounds, that adding and subtracting a vortex would give the same response.

We have also tried varying the strength of the inductive coupling constant λ_J^2, considering $\lambda_J^2=0.01$, 0.1, and 10.0 as

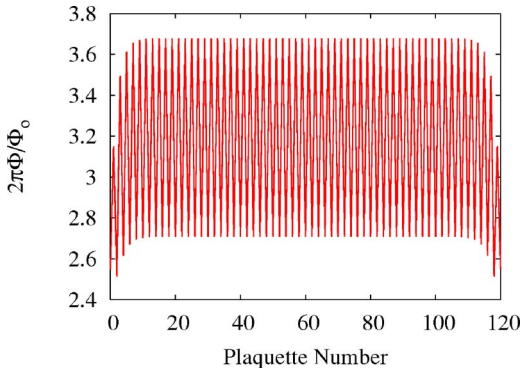

FIG. 11. (Color online) Normalized flux vs plaquette number, plotted for $N=121$ and $f=61/121$.

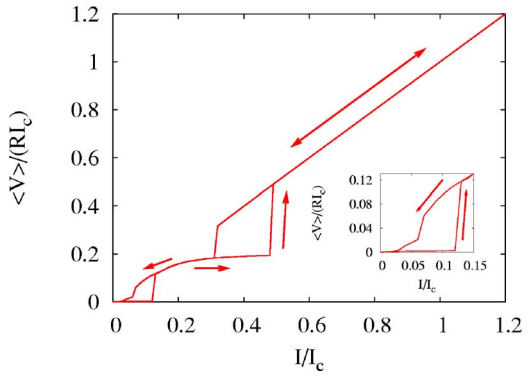

FIG. 12. (Color online) I-V characteristics for $N=121$ and $f=61/121$, for the parameters of the preceding figure. Inset: enlargement of I-V characteristics at small currents.

well as 1 for $f=1/2$. For $\lambda_J^2=0.01$, the system behaves like a collection of independent junctions: $\langle V\rangle=0$ for all $I/I_c<0.9$, and the flux pattern is very similar to that of Fig. 4. $\lambda_J^2=0.1$ also gives results very similar to those of Fig. 4. But for $\lambda_J^2=10$, the fluxons are depinned even at $I/I_c=0$, and the I-V curve is very similar to that seen in Ref. 24 for a long junction in the continuum limit. We have also carried out calculations (not shown here) for values of $Q_J=1.0$, 5.0, and 50.0 for $f=1/2$, $N=120$, and $\lambda_J^2=1.0$. The position of the first jump in the I-V curve remains unchanged even for the critically damped case ($Q_J=1.0$). We found that, for the larger Q_J's, the fluxons are expelled from the ladder at lower currents than for smaller Q_J's. Finally, for $Q_J=1.0$, the I-V curve of the ladder closely resembles that of a single small, critically damped junction.

H. $f=1/2+1/(2N)$: One added half fluxon

As a final calculation, we have considered a ladder with an *odd* number of plaquettes, namely $N=121$, and $f=61/121$. Intuitively, one might expect that this ladder would correspond to a single added 1/2 fluxon superimposed on an $f=1/2$ ground state. The latter corresponds to $f=1/2=60.5/121$, while the extra 1/2 fluxon is needed in order to bring the total flux up to $f=61/121$. Indeed, the flux plot, shown in Fig. 11, is consistent with this picture: an alternating flux pattern of the $f=1/2$ ground state on which is superimposed the flux pattern of a *single* 1/2 fluxon, i.e., one of the two excitations distinguishable in Fig. 6.

The I-V characteristics of this ladder (shown in Fig. 12), are consistent with this picture. There are three regimes of nonzero voltage (seen most clearly on the decreasing current branch), namely (i) motion of the 1/2 fluxon through the background of the pinned $f=1/2$ lattice; (ii) motion of the depinned $f=1/2$ lattice; and (iii) purely resistive behavior, with all small junctions in the voltage state. The motion of the half fluxon [in regime (i)] is particularly intriguing. At a given current, the voltage generated by this 1/2 fluxon is $\sim 1/2$ that produced by the two moving 1/2 fluxons at the corresponding current in Fig. 6. This result is consistent with the picture that the two 1/2 fluxons in Fig. 6 move at the same average velocity at any given applied current. In addition, as mentioned earlier, at all currents in this regime, the time-averaged voltage $\langle V\rangle$ generated by the 1/2 fluxon is related to the ac frequency ν of that voltage by

$$\frac{\langle V\rangle}{RI_c}=\frac{\pi}{NQ_J\Delta\tau}, \tag{13}$$

where $\Delta\tau=\omega_p/\nu$. As an illustration, we show in Fig. 13 $V(\tau)/(RI_c)$ for $f=61/121$ and a ladder of length 121 plaquettes, at a current $I/I_c=0.03$, in the regime where the voltage is produced by a single 1/2 fluxon.

IV. DISCUSSION

We have shown that a single fluxon introduced into a Josephson ladder will fractionalize if the ladder is initially in an $f=1/q$ ground state with $q=2$, 3, 4, 5, or 6. This fractionalization leads to a characteristic behavior of the (suitably defined) flux in the ground state at $I/I_c=0$, and even for $I/I_c\neq 0$, provided that I is smaller than the critical current for onset of voltage. Once a measurable voltage is obtained across the ladder, for these fields, there is a characteristic series of regimes with increasing current: first, the fractionalized fluxon moves, generating a voltage; then, the underlying fluxon lattice is depinned; and finally, the ladder as a whole switches to the voltage state and the fluxons are expelled from the ladder.

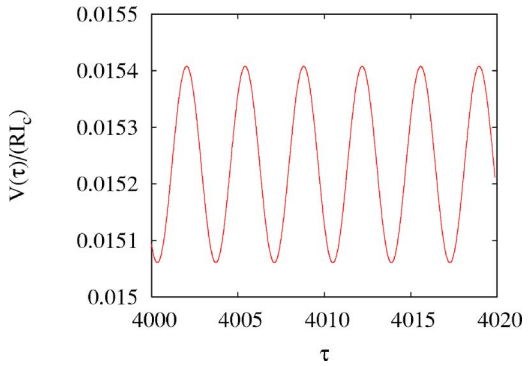

FIG. 13. (Color online) Time-dependent voltage $V(\tau)/(RI_c)$ plotted for dimensionless time τ between 4000 and 4020, for f $=61/121$ and current $I/I_c=0.03$. $Q_J=10$ and $\lambda_J^2=1$. The dimensionless period of oscillation $\Delta\tau$ satisfies Eq. (13).

The type of fractional excitation found here are basically walls between different domains of the underlying $1/q$ ground state. For an applied field of $1/q$, there are q discrete flux lattice ground states, each shifted by one plaquette from the next ground state. If two different ground state domains, shifted by one plaquette, are placed next to one another, a $1/q$ fractional fluxon is formed. Such walls, with fractional vortex charge, are the analogs of fractional excitations well known in many other physics contexts, especially in one dimension. For example, solitons in polyacetylene are fractionally charged excitations which can form between two domains of alternating singly and doubly bonded carbons in this one-dimensional chain compound.[25] The fractional fluxons in the Josephson ladder are unusual because it appears that a fluxon of *any* rational fraction can form in a suitable applied magnetic field.

The fractional vortices described in this paper generally produce a *nonhysteretic I-V* characteristic, even if the individual junctions which make up the ladder are hysteretic. This behavior is similar to that previously observed for integer vortices in two-dimensional arrays,[26] which also move in a nonhysteretic fashion even when the junctions in the array are hysteretic. In the case of the two-dimensional (2D) arrays, the explanation for this behavior is that the effective quality factor describing the voltage generated by the moving vortex is $Q_{eff}=(2eR^2I_dC/\hbar)^{1/2}$, where C is the junction capacitance, R is the junction shunt resistance, and I_d is the current required to depin a vortex from its equilibrium position within a plaquette of the 2D lattice. Since $I_d \sim 0.1I_c$ in the 2D case, where I_c is the critical current of one junction, Q_{eff} is much smaller than the junction quality factor $(2eR^2I_cC/\hbar)^{1/2}$, and hence, the motion of the vortex is overdamped even when the individual junctions are underdamped and hysteretic.

For the ladder arrays, the depinning current I_d for a fractional fluxon is less than $0.01I_c$ for all cases we have considered in this paper. Hence, even though $Q_J=10$, the analogous effective quality factor for the fractional fluxon will be less than 0.1. The resulting *I-V* characteristics should thus be nonhysteretic and similar to those of an overdamped Josephson junction, as we have observed numerically (see Fig. 13). However, we have not succeeded in deriving a driven-pendulumlike equation of motion for the fractional vortex, similar to that given in Refs. 23 and 26.

One striking feature of these fractionalized fluxons is that they do *not* appear to form in two dimensions. When a fluxon is added to an $f=1/2$ ground state of a square lattice in two dimensions, the fluxon is depinned at a current much lower than that of the $f=1/2$ lattice, just as in one dimension. However, numerical studies suggest that the fluxon is not fractionalized, but remains a compact object.[26] Fractionalization is apparently easier in one dimension (1D) because the domain walls are zero dimensional, and hence, require much lower energy to form.

It is of interest to compare this prediction to what we would expect from a single *unfractionalized* fluxon in an otherwise empty ladder. Here, the expected mechanism of fluxon motion is that the fluxon moves by one plaquette. An argument similar to that just given yields $\langle V\rangle=[h/(2eN)\nu$.

We can also consider the motion of an unfractionalized vortex through the background of a pinned $f=1/q$ fluxon lattice. Since the motion of the single vortex would have a period of q lattice constants, and since there would be a phase slip of 2π each time the vortex circulates once around the ladder, the equation relating the time-averaged voltage to the period would be $\langle V\rangle/(RI_c)=2\pi q/(Q_J\Delta\tau)$, where $\Delta\tau$ is the period of the ac voltage, in units of $1/\omega_p$. This relation is the same as would hold for a vortex fractionalized into q parts and moving through the same background.

Thus, the clearest experimental way to see a signature of the fractionalization would be to compare the period of the ac voltages with the time-averaged voltage in a ladder with *isolated* fractional vortices. Such ladders were discussed earlier—an example is the case of $N=121$ and $f=61/121$, which contains a single $1/2$ fluxon in a background of an $f=1/2$ fluxon lattice. Besides searching for a signal of the fractionalized vortices in the *I-V* characteristics, perhaps the flux profile of the fractionalized vortices could also be directly imaged.

As mentioned earlier, the fractional vortices discussed here were previously suggested[16] for a ladder of alternating 0 and π junctions. Since fractional vortices can thus appear in both types of ladders, one might ask if any information about the nature of the junctions (i.e., whether they are 0 or π junctions) could be gleaned from a simple inspection of the *I-V* characteristics. If *all* the rungs of the ladder are π junctions, they would have the same *I-V* characteristics as a ladder made entirely of 0 junctions, since the presence of π junctions would produce no additional frustration in this case. Thus, the *I-V* characteristics would not distinguish between all 0 and all π junctions. If the ladder contained alternating 0 and π junctions, the *I-V* characteristics, in the presence of a magnetic field, would differ from that for all 0 (or all π) junctions by being shifted in magnetic field by $1/2$ a flux quantum per plaquette—that is, the *I-V* characteristics of the alternating ladder at field f would be the same as that of the 0 or π ladder at $f+1/2$. For a more complicated distribution of 0 and π junctions, the *I-V* characteristics of the ladder would be more complicated, and the presence of fractional vortices might be difficult to detect. Thus, the existence of fractional vortices, of itself, might not be sufficient to determine if the ladder were partly composed of π junctions.

Finally, we note that the present results are all obtained from a classical set of governing equations. If the individual junctions are sufficiently small, we expect that the fractional fluxons would behave like quantum-mechanical particles. Specifically, the phase configuration of the ladder would be described by an N-dimensional wave function $\Psi(\phi_1,\ldots.\phi_N)$, which would be an eigenfunction of the ladder Hamiltonian (expressed as an operator). It would be of interest to calculate the spectrum of such eigenstates, and to study the behavior of a lattice, in the small junction regime, containing two or more such quantum-mechanical fractional fluxons. One important question would be the statistics (Bose, Fermi, or fractional) obeyed by such particles. Such questions, though fascinating, are, however, beyond the scope of the present paper. In addition, there should be a broad range of experimental parameters where the classical equations are applicable. Thus, the present predictions should be readily testable experimentally.

ACKNOWLEDGMENTS

We are grateful for valuable conversations with R. V. Kulkarni, who called our attention to Ref. 16, and to E. Almaas. This work was supported by NSF Grant No. DMR 04-13395; calculations were carried out using the facilities of the Ohio Supercomputer Center.

*Electronic address: itornes@mps.ohio-state.edu
†Electronic address: stroud@mps.ohio-state.edu

[1] P. Binder, D. Abraimov, A. V. Ustinov, S. Flach, and Y. Zolotaryuk, Phys. Rev. Lett. **84**, 745 (2000).
[2] L. M. Floria, J. L. Marin, P. J. Martinez, F. Falo, and S. Aubry, Europhys. Lett. **36**, 539 (1996).
[3] M. Kardar, Phys. Rev. B **33**, 3125 (1986).
[4] P. Binder, D. Abraimov, and A. V. Ustinov, Phys. Rev. E **62**, 2858 (2000).
[5] S. Flach and M. Spicchi, J. Phys.: Condens. Matter **11**, 321 (1999).
[6] J. J. Mazo, F. Falo, and L. M. Floria, Phys. Rev. B **52**, 10433 (1995).
[7] C. Denniston and C. Tang, Phys. Rev. Lett. **75**, 3930 (1995).
[8] E. Trias, J. J. Mazo, A. Brinkman, and T. P. Orlando, Physica D **156**, 98 (2001).
[9] E. Granato, Phys. Rev. B **42**, R4797 (1990).
[10] J. J. Mazo, E. Trias, and T. P. Orlando, Phys. Rev. B **59**, 13604 (1999).
[11] P. Caputo, M. V. Fistul, B. A. Malomed, S. Flach, and A. V. Ustinov, Phys. Rev. B **59**, 14050 (1999).
[12] S. Ryu, W. Yu, and D. Stroud, Phys. Rev. E **53**, 2190 (1996).
[13] M. Barahona, S. H. Strogatz, and T. P. Orlando, Phys. Rev. B **57**, 1181 (1998).
[14] B. R. Trees and N. Hussain, Phys. Rev. E **61**, 6415 (2000).
[15] W. B. Yu, E. B. Harris, S. E. Hebboul, J. C. Garland, and D. Stroud, Phys. Rev. B **45**, R12624 (1992).
[16] M. Chandran and R. V. Kulkarni, Phys. Rev. B **68**, 104505 (2003).
[17] J. J. A. Baselmans, A. F. Morpurgo, B. J. van Wees, and T. M. Klapwijk, Nature (London) **397**, 43 (1999); J. J. A. Baselmans, B. J. van Wees, and T. M. Klapwijk, Phys. Rev. B **63**, 094504 (2001).
[18] T. Lofwander, V. S. Shumeiko, and G. Wendin, Supercond. Sci. Technol. **14**, R53 (2001).
[19] V. V. Ryazanov, V. A. Oboznov, A. Yu. Rusanov, A. V. Veretennikov, A. A. Golubov, and J. Aarts, Phys. Rev. Lett. **86**, 2427 (2001).
[20] See, e.g., M. Tinkham, *Introduction to Superconductivity*, 2nd ed. (McGraw-Hill, New York, 1996), pp. 202–213. The coupled RCSJ model has been used by many authors to treat the dynamics of Josephson junction arrays; some examples are S. R. Shenoy, J. Phys. C **18**, 5163 (1985); F. Falo, A. R. Bishop, and P. S. Lomdahl, Phys. Rev. B **41**, 10983 (1990); R. Bhagavatula, C. Ebner, and C. Jayaprakash, *ibid.* **45**, R4774 (1992).
[21] W. H. Press, S. A. Teukolsky, W. T. Vetterling, and B. P. Flannery, *Numerical Recipes in C* (Cambridge University Press, Cambridge, 2002), pp. 707–747.
[22] See, e.g., S. Ryu and D. Stroud, Phys. Rev. Lett. **78**, 4629 (1997), for an explicit definition of the vortex number.
[23] M. S. Rzchowski, S. P. Benz, M. Tinkham, and C. J. Lobb, Phys. Rev. B **42**, 2041 (1990).
[24] I. Tornes and D. Stroud, Phys. Rev. B **71**, 144503 (2005).
[25] W. P. Su, J. R. Schrieffer, and A. J. Heeger, Phys. Rev. Lett. **42**, 1698 (1979); Phys. Rev. B **22**, 2099 (1980).
[26] W. Yu, K. H. Lee, and D. Stroud, Phys. Rev. B **47**, 5906 (1993).